JOURNAL OF OPTOELECTRONICS AND ADVANCED MATERIALS Vol. 9, No. 1, January 2007, p. 106 - 113

Invited Lecture

"Micromorph" tandem solar cells at high deposition rates

J. K. RATH
Utrecht University, SID-Physics of Devices, P.O. Box: 80000, 3508 TA Utrecht, The Netherlands

In this paper, three aspects that are necessary for the successful fabrication of μc-Si cells at high deposition rates are dealt with; (i) innovative growth processes such as deposition by plasma CVD at very high frequencies and high pressure depletion (HPD) conditions (ii) in-situ gas phase as well as growth diagnosis and (iii) cell engineering. The paper also describes various new concepts such as the application of an external DC bias to the cathode and application of a nonlinear grading during deposition, that would among others reduce the ion energy and improve the structure of the film respectively. The light induced degradation characteristics of the μc-Si cells in comparison to a-Si and proto-Si are discussed. The recent developments of single junction μc-Si solar cells and micromorph tandem cells at Utrecht University, such as world's highest stabilized efficiency of 10% at a deposition rate of 0.5nm/s, an efficiency of 6.7% at 5nm/s for μc-Si and 11.4% (12% initial) for micromorph cells made in a superstrate configuration are presented. Whereas the μc-Si showed improvement with light soaking, the tandems suffered only a 5% loss in efficiency.

(Received November 28, 2006; accepted December 21, 2006)

Keywords: Thin films, Electrical properties, Computer simulation, Guinness

1. Introduction

Tandem type thin film solar cells consisting of series connected amorphous silicon (a-Si:H) as the top cell and microcrystalline silicon (μc-Si) as the bottom cell are now considered to be the most promising types of device for achieving stabilized efficiencies greater than 15%. Many industries, such as Unisolar (US), Kaneka Corp (Japan) and Mitsubishi (Japan) are now devoted to this concept. The indirect band gap nature of the μc-Si material and the need for sufficient absorption in the long wavelength part of the solar spectrum demand rather thick layers to be used in solar cells. Thus the deposition rate (Rd) of the μc-Si has become the focal point of research into the development of micromorph solar cells.

Micromorph thin film silicon solar cells (amorphous/microcrystalline silicon tandem cells) have proven to be a good alternative to the completely amorphous multijunction cells consisting of amorphous silicon and silicon germanium. However, after the initial excitement over the success of the Neuchatel group on these new high efficiency cells [1], a great deal of discussion concerning the real superiority of the micromorph cell in comparison with the amorphous silicon type cells containing silicon germanium has taken place. This has predominantly arisen due to the rather thick bottom cells used in micromorph devices, and the efficiency of microcrystalline cells tends to decrease monotonically with increasing deposition rate [2]. A related problem, of course, arises that in these high current generating cells, the top cells also become thicker. This means we have to deal with two issues. The first and most important one is the deposition rate of the bottom cells (microcrystalline cells). I will show here how high deposition rate microcrystalline silicon cells are made by very high frequency plasma enhanced chemical vapour deposition (VHFPECVD) and what are the basic issues. The second issue is to implement suitable amorphous materials for the top cell. In this respect, we have implemented first a VHF PECVD material with a moderate deposition rate (0.2 nm/s). Next, a high deposition rate top cell (1 nm/s) is implemented. The idea behind these types of cell is that with very stable bottom cells, the choice of top cells is rather flexible, provided that the bottom cells are current limiting in the tandem cell structure. In this paper, mainly the results obtained with VHF PECVD at Utrecht University (UU) are described. However, the results from other deposition techniques such as HWCVD are also briefly given, to explore other possibilities.

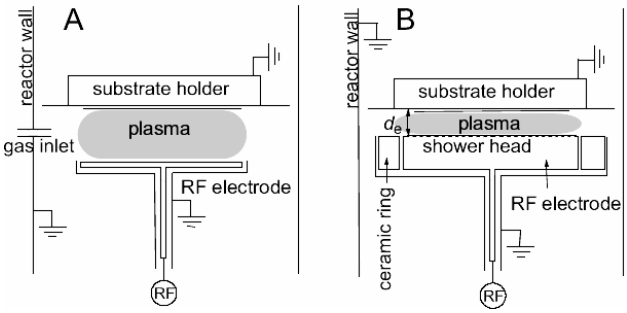

Fig. 1 . The RF electrodes used for amorphous (A) and microcrystalline (B) depositions in ASTER.

2. Experimental

Deposition of amorphous silicon and microcrystalline silicon layers have been carried out in a UHV multichamber system called ASTER [3] that has four

process chambers. We employ two types of electrode (Fig. 1) to deposit amorphous silicon and microcrystalline silicon respectively. Electrode A is used for the deposition of amorphous silicon layers for the implementation of the top cell of the tandem structure. The frequency of the RF power for this case is variable up to 100MHz, and the maximum power that can be delivered is 100W. However, for the deposition of a-Si:H reported in this article, the frequency is fixed at 50MHz. The electrode B that is used for microcrystalline layer deposition can have a variable position, and the distance between the electrodes can be made rather small (down to 5mm) to adapt to the high process pressure conditions. Power up to 1000W from an RF generator with a frequency 60MHz is fed to the electrode B. The microcrystalline silicon i-layers reported in this study have been made with an electrode distance of 6 mm, at an estimated substrate temperature of 180 ^{o}C, using a moderate hydrogen dilution of the silane gas that delivers the material at the transition from the microcrystalline to the amorphous state. The dilution is expressed as $d_H=fH_2/fSiH_4$. The optical emission of the plasma (due to transitions from excited states of molecules that are formed due to electron impact reactions) is detected through a quartz window view port. An Avantes MC2000 calibrated CCD spectrometer is used to record the spectrum. A lens system and fiber optics are used to focus on the emission from the pre-sheath region near the substrate. The spectral resolution is of the order of 1 nm; integration times of around 0.5 s are required. By means of a calibration routine, the spectra are corrected for the decreasing transmission of the quartz window due to the deposition on the window. With optical emission spectroscopy (OES), the intensity of the Si* line (289 nm) and the Balmer alpha (H_α) line (656 nm) are recorded and analyzed.

The crystallinity of the deposited material is estimated using Raman spectroscopy. The crystalline ratio R_c was obtained as

$$R_c = \frac{I_{520} + I_{510}}{I_{480} + I_{520} + I_{510}} \quad (1)$$

where I_{520} and I_{510} are the intensities of the crystalline contribution whereas I_{480} is that of the amorphous contribution to the transverse optical Si–Si vibrations in the Raman spectra. The details of the deconvolution procedure and the evaluation of the Raman crystalline fraction has been reported previously [4]. The value of R_c is underestimated compared to actual crystalline volume fraction X_c. The thickness of the samples has been measured by a step surface profiler and reflection/transmission measurements.

3. Results and discussion

3.1. Amorphous silicon

As mentioned in the introduction, the high current generating nature of the microcrystalline silicon bottom cells necessitates a rather high current generation of the top cell for current matching. Thus, a rather thicker top cell is needed and this demands high stability of the material. Generally, stable amorphous silicon films are made at the transition regime of growth (also know as the protocrystalline condition), in which case a widening of the band gap is observed that leads to lower absorption strength [5]. Thus, thicker material is needed to deliver the desired current in the top cell.

The deposition rate in a PECVD process can be increased substantially by increasing the power, as long as the deposition is in the non-depletion regime (i.e., by simultaneously increasing the gas flow rate of the silicon containing precursor). However, it has to be ensured that the deposition does not enter into the so called γ' regime (also called the dusty regime) [6]. One of the solutions to this problem is to adapt the deposition process by applying modulation to the amplitude of the RF voltage.

3.1.1 VHF - PECVD

The deposition rate of amorphous silicon (and also microcrystalline silicon) is a function of the electron density in the plasma. Changing the frequency of the RF plasma leads to a change in the electron density, and it has been shown that application of a high frequency is one of the ways to increase the electron density and hence the deposition rate. In the case of VHF PECVD, a monotonic increase in the deposition rate with increasing frequency has been observed [7]. However, this effect is somewhat compensated by a power loss in the feed though and cables at high frequencies.

One of the ways to increase the deposition rate is to increase the pressure, while adjusting the regime of the growth in such a way as to keep the residence time short enough to avoid higher radicals or dust formation. Cannon has, using such a method, been able to achieve 2nm/s [8].

At UU, a different approach has been made to increase the deposition rate. It has been observed that application of an amplitude modulation to the RF plasma changes the deposition rate, and a monotonic increase of deposition rate with increasing modulation up to 100 KHz has been observed (Fig.2) [9]. The deposition rate at the optimum modulation is more than 4 times higher than for RF power without modulation. A deposition rate of 0.89nm/s for a gas flow of 30/30 (sccm) SiH_4/H_2 flow has been reached [9]. This has been attributed to the heating of the electrons at the onset of the on cycle of the modulation. Kinetic OES measurements confirm this. By depositing in the γ' regime with increasing pressure, a deposition rate of 1nm/s has been achieved [10].

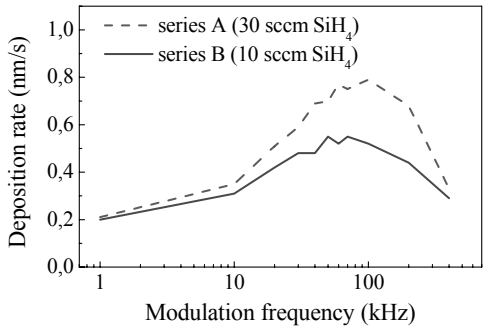

Fig. 2: Variation of the deposition rate of an a-Si:H film with modulation frequency, for VHF PECVD deposition [9].

Another outcome of the amplitude modulation is the improvement of the homogeneity of deposition. On a 10x10 cm^2 substrate across an area with diameter of 7.2nm, an inhomogeneity of <7% has been achieved [9] at the optimum modulation of the RF voltage (Fig.3). This effect has been attributed to heating of the plasma across the plasma volume.

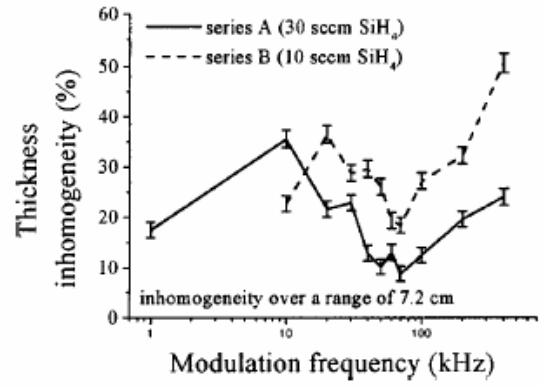

Fig. 3. Dependence of inhomogeneity on the modulation frequency of the RF amplitude [9].

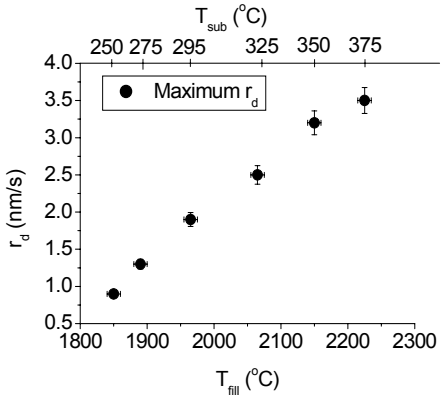

Fig. 4. Variation of the deposition rate of an a-Si:H film with the filament temperature, in HWCVD deposition [14]

A third benefit of the amplitude modulation is an improvement in the gas use, which is further enhanced by decreasing the total gas flow. A combination of amplitude modulation at 100 KHz and a gas flow of 10/10 sccm SiH_4/H_2 gas flow delivers ~ 50% of the gas use [11].

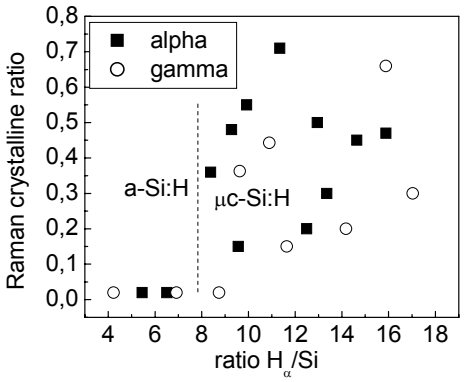

Fig. 5. Dependence of the Raman crystalline fraction on the H_α/Si^* [32].

Amorphous silicon made by amplitude modulation maintains excellent device quality, even with the increased deposition rate. The material made at 0.89nm/s shows a photosensitivity of > 10^6 and a defect density of < $10^{16}/cm^3$. An n-i-p cell with this i-layer, made by amplitude modulation with VHF PECVD, delivered an efficiency of 6.8%, even without application of a back reflector [12]. This translates to an efficiency of ~ 10% if a back reflector is used (considering a ~ 40% increase in the current due to a back reflector). This is a respectable value for a deposition rate that is close to 1nm/s.

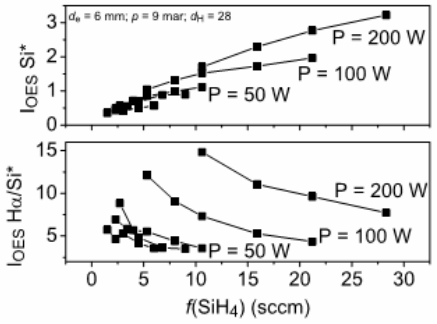

Fig. 6 . Dependence of the 1) intensity Si^* and 2) intensity ratio ($H\alpha/Si^*$) on the RF power and gas flow rate [33].

3.1.2 Other techniques

An alternative deposition method is the use of hot-wire CVD (also called Cat-CVD). This is an ion free deposition; a dust free deposition is assured even at high deposition rates. This technique also can deliver a high deposition rate and shows high gas use. The high deposition rate can simply be achieved by increasing the filament current and the gas flow simultaneously. At UU,

a protocrystalline type of material (an amorphous type material with increased medium range order) has been achieved at a deposition rate of 1nm/s at a substrate temperature of ~ 250 °C. Whereas structural studies confirm its protocrystalline character, light soaking studies shows good stability [13]. The deposition rate of > 3nm/s has been achieved by increasing the filament temperature [14], which is always accompanied by an increase in the substrate temperature (as no artificial cooling of the substrate is applied). An initial efficiency of 7.5% has been achieved at a deposition rate of 3.2nm/s (Fig. 4).

Expanding thermal plasma (ETP) and Microwave PECVD are also possible candidates for high deposition rates, although high efficiency cells by these techniques are yet to be realised. An initial efficiency of 8% [16] has been achieved at TU Delft with a p-i-n cell incorporating an ETP grown a-Si:H i-layer made at 1.1nm/s. However, the cell suffers a very high degradation of ~40% with light soaking. Table I shows the state of the art efficiencies achieved by various groups for p-i-n or n-i-p solar cells at high deposition rates.

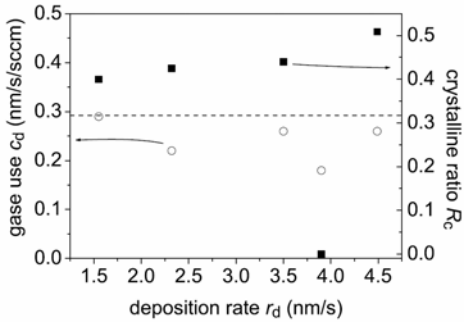

Fig. 7 . Correlation between gas use and the crystalline ratio in a microcrystalline silicon material at various deposition rates. The case of a material with a low gas use at 3.9nm/s has a drastic effect on the crystallinity in the material [30].

Table 1. Reported efficiency values for amorphous silicon solar cells at high deposition rates.

Univ./Inst./Comp.	η(%) (initial)	η(%) (Stabl)	Rd (nm/s)	Technique	speciality	Ref
Osaka Uni/Sanyo/Sharp	8.25 (pin)		128.1	VHF	Atm Press	17
Mitsubishi Heavy Industrie	8 (pin)		1.0	VHF		18
Canon/NIAIST	9.3(nip)	8.2	2.0	VHF		8
NREL	9.8 (nip)	7.7	1.8	HWCVD		19
Kyocera	10.1	8.2	2.8 0.8	HW/PECVD		20
UU	6.5 (SS nip)		0.8	AMVHF	Without BR	12
UU	7.5 (SS nip)		3.2	HWCVD		15

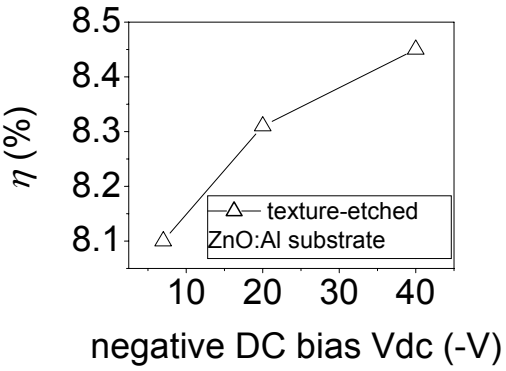

Fig. 8. Dependence on external dc bias during deposition of the efficiency of a p-i-n microcrystalline silicon solar cell. [35].

3.2 High growth rate microcrystalline silicon

The success of microcrystalline silicon solar cells can be attributed to identifying the following regimes of growth; (1) control of ion energy which is achieved by depositions at high frequency and/or high pressure, (2) materials made at the transition to amorphous growth. Control of the ion energy becomes especially critical for deposition at high rates. A deposition regime called high pressure depletion (HPD) [21] shows how this can be achieved.

In 1996, the author proposed that microcrystalline silicon can be made in different regimes, and two specific regimes of growth had been identified as important for device performance [22]. These two types were named Poly1 and Poly2. Whereas Poly1 is a material made at high hydrogen dilution and is completely crystalline with no noticeable amorphous incubation, it is very defective and porous, characterised by typical 2100 cm^{-1} modes of vibration in the IR spectrum, and goes through fast post deposition oxidation (becomes n-type). Poly2 type films, on the other hand, are made at low hydrogen dilution (in the particular case H_2/SiH_4 =10 [23]) near to the amorphous transition regime. A further reduction in dilution basically leads to an amorphous matrix with crystalline islands dispersed in it [23]. Poly2 type material made at low hydrogen dilution has the characteristics of a compact structure and the hydrogen atoms in the film are at compact sites [24] (2000 cm^{-1} in the IR spectrum [25]). These sorts of material showed the device quality, but suffered from an amorphous incubation phase, being in a deposition regime near the transition. Thus, a deposition of Poly2 with Poly1 seed (called a profiled layer) was proposed, which delivered the first working cell by HWCVD with reasonable efficiency (4.41%) [26]. Subsequently it was established by the Julich group [27],

and then by others [28,29] that indeed a transition type material made at the microcrystalline to amorphous transition delivers the best cell performance.

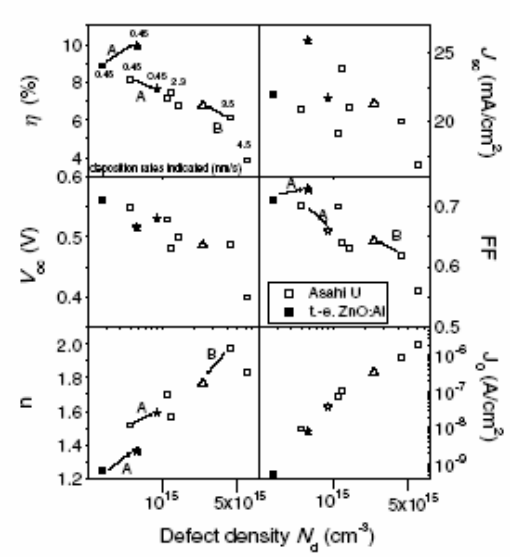

Fig 9. Solar cell data versus FTPS defect density for μc-Si:H solar cells made at various deposition rates, hydrogen source gas dilution, deposition temperature and applied external DC bias voltage. Arrows A indicate an increase in hydrogen dilution (at a deposition rate of 0.45 nm/s); arrows B indicate the application of an external DC bias voltage of -20 V. The open symbols are for Asahi U-type substrates with a ZnO protection layer and closed symbols are for texture-etched ZnO substrates. Stars indicate high dilution and triangles indicate DC biased. [34].

3.2.1 VHF-PECVD

At UU, we have used a deposition process in the HPD regime combined with VHF and a shower head for gas distribution in the plasma zone. A number of deposition parameters (such as pressure, power and gas flow rate) have to be adjusted to achieve device quality microcrystalline silicon at high deposition rates [30] and for this, the quality control of the silicon material is very crucial. The quality control has been made in several ways. The main method is monitoring the crystalline fraction of the material by Raman spectroscopy. We have observed that the crystalline component is a major deciding factor on the photosensitivity of the material, and the solar cell behaviour depends sensitively on the crystalline fraction. The material in the microcrystalline to amorphous transition regime delivers the most desired characteristics, and we have found that an $R_c \sim 0.4$ is the best [31]. Therefore, we have meticulously maintained this fraction in the material, when comparing the behaviour of solar cells with i-layers made under different deposition conditions. We have always measured the Raman spectra at the front and back sides of the microcrystalline silicon films, to know the evolution of the crystallinity in the growth direction. For the case of a complete solar cell, this method, though not very accurate owing to the influence of the doped layers, is very helpful for the quality control of the i-layer in the cell. As the crystallinity increases with thickness, when no grading to hydrogen dilution is applied, the average crystalline fraction in the material is the property that is monitored.

Two other techniques have been employed to control the quality of the microcrystalline silicon i-layer in the solar cell, in addition to looking at the Raman crystalline fraction. The first is optical emission spectroscopy. For plasma conditions aiming for transition type μc-Si, we have monitored the intensity of the Si^* and the intensity ratio H_α/Si^*. The ratio H_α/Si^* in the emission spectrum of the plasma is a fingerprint of the phase of the deposition [32] and the amorphous to crystalline transition can the monitored (Fig. 5). Figure 6 (1) shows the variation of the Si^* intensity as a function of the silane flow (d_H is kept constant at 28). In these series, all the materials are made at a constant hydrogen dilution that is near to the transition regime of growth. It can be seen from Fig. 8 that at each power the Si^* intensity increases linearly with increasing silane flow, which is an indication that the silane is highly depleted. Fig. 6(2) shows the dependence of the H_α/Si^* ratio with silane flow rate (keeping d_H constant at 28) at a series of increasing powers. It can be observed that at each power, an increase in the silane flow rate leads a decreasing H_α/Si^* ratio, which is attributed to the loss of hydrogen due to an abstraction reaction with the silane gas in the gas phase. Hence, following the trend from Fig. 6(1), if we simply increase the silane gas flow keeping the dilution constant, we will end up with amorphous silicon due to the lowering of the H_α/Si^* ratio. It is seen from Fig. 7 that the power has to be proportionately increased to maintain the H_α/Si^* ratio. The key parameter is to maintain the depletion. In addition we have introduced a new parameter (explained below) which gives better control of the depletion condition.

We have observed that as the deposition rate is increased (increasing the power and total gas flow (keeping the d_H constant)), maintaining this ratio is itself not sufficient to achieve the desired crystallinity. So we have introduced another technique to accurately find a parameter to describe the optimum deposition conditions. We call this the "gas utilisation parameter" [30]. This quantity is defined as c_d = deposition rate/silane gas flow rate, which basically is a measure for the depletion condition. We have seen that by just increasing the power and gas flow in the same proportion (for example from 50W at 2.3nm/s to 100W at 3.5nm/s), it is not possible to maintain the same depletion condition, and the c_d is reduced (Fig. 7 for r_d = 3.9 nm/s). This is manifested by the lowering of the crystallinity in the film (see in Fig. 7 for r_d = 3.9 nm/s). By adjusting the total flow rate, the depletion can be maintained at a desired level (which is estimated in our case to be 0.29 nm/s/sccm) and the required crystalline fraction is restored. For the deposition at 200W and 400W we again employed this method of adjusting the flow to maintain the desired depletion. We think this new gas utilization parameter is an important

concept for depositions in the high pressure depletion regime. The result of this is that we have been able to produce microcrystalline silicon materials with device quality, even up to a deposition rate of 4.5nm/s. The quality of this layer is confirmed from the low defect density, of the order of 10^{15} cm^{-3} [34], measured by Fourier transform photocurrent spectroscopy (FTPS) (Fig. 9).

3.2.1a. External dc bias

The first adaptation that we made to the standard deposition under high pressure depletion conditions is the application of an external bias to the cathode, which effectively reduces the plasma potential and the ion energies, without changing the gas phase chemistry significantly [35]. The characteristics of the gas phase composition of the species has been monitored by OES, which shows that there is little change in the Si^*/H_α ratio (that has a strong correlation with the growth kinetics).

Fig. 8 shows the voltage dependence of the IV parameters (efficiency) of a p-i-n microcrystalline silicon solar cell with external dc bias. The FF also follows this trend. From FTPS measurements on real solar cells, it was clearly observed that the defect density systematically decreases (Fig. 10) with increasing (negative) external bias voltage to the cathode during deposition. A reduction by a factor of two in the defect density is obtained by applying a voltage of 20V.

3.2. 1b. Grading of hydrogen dilution

The second concept is the use of a parabolic grading [35] of the hydrogen dilution used for the deposition of the i-layer.

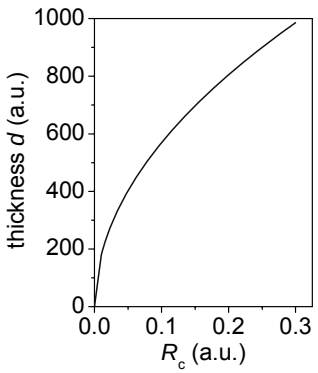

Fig. 10. Conical growth of crystallites leads to quadratic growth of crystalline volume fraction when material is deposited with constant hydrogen dilution [35]

The microcrystalline material normally grows in an inhomogeneous way, i.e., incubation, nucleation and then conical growth to reach the full crystalline region at some thickness. Fig 10 shows the crystalline fraction at different thicknesses of the microcrystalline silicon material made at constant hydrogen dilution ($H_2/(SiH_4+H_2)$). There is a quadratic increase in the crystallinity with increasing thickness. Thus, for very thick films, the material at the top end becomes highly crystalline and is not at the optimum condition of transition type material. To overcome this problem, the development of the crystallinity in the growth direction was retarded by using a parabolic type of grading, where the hydrogen dilution was step-wise reduced to maintain the crystallinity at a constant level. This concept allows us to obtain homogeneous growth of the i-layer, confirmed by comparing the Raman spectra obtained from the top (n) and bottom (p) side of the microcrystalline silicon cell. Fig 11 shows the IV parameters of pin microcrystalline silicon solar cells at different thicknesses, made with and without parabolic grading. It is observed that with constant grading, the efficiency suffers considerably when the thickness is increased from 1 to 2 microns. The beneficial effect of grading for the thicker i-layer is clearly observed.

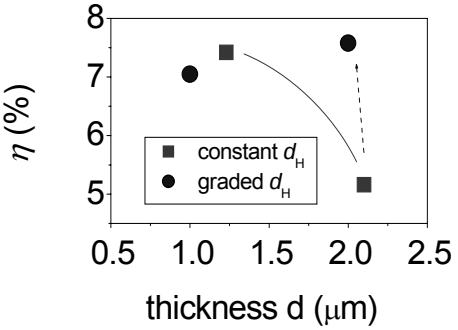

Fig. 11. Thickness dependence of solar cell parameters (average best 10) for i-layers deposited with a constant as well as a parabolic graded hydrogen dilution [35].

3.2.2 High efficiency microcrystalline silicon cells

We have shown the world's highest stabilized efficiency (10 %) [31] for microcrystalline silicon cells. Moreover, a microcrystalline silicon p-i-n cell with stabilized efficiency of 6.7 % has been achieved at high deposition rate of 4.5nm/s [30]. These cells show a particularly interesting behaviour in that the efficiency actually improves with light soaking (Initial efficiency of 6.4% leads to 6.7% with light soaking) [30]. This makes them very useful as current limiting cells of a tandem cell. In addition, this effect makes the choice of the top cell more flexible (if the tandem cell is bottom cell limiting).

3.2.3 Other techniques

Among other techniques, besides standard RF PECVD [13.56 MHz] made with high pressure condition, only HWCVD shows promise (4.4% efficiency at 1.1nm/s for n-i-p cell on SS substrate without a BR) [36]. Hybrid type of HWCVD+PECVD (by Kyocera) deposition also shows promising efficiencies at high deposition rates.

3.3 Micromorph cells

When our best (10% efficiency) microcrystalline silicon cells are implemented as bottom cells, they deliver state-of-the-art tandem cells with efficiencies that are among the best in the world. Here, the deposition rate of the microcrystalline silicon cell is moderate (0.45nm/s). The top cell uses standard amorphous silicon made at 200 ^{o}C with a flow ratio SiH_4:H_2=1:1 that delivers an efficiency ~ 10% in a p-i-n cell on an Asahi U-type substrate. The thickness of the top and bottom cells of the micromorph cell presented here are ~ 300 nm and ~ 1.5 microns respectively. In this configuration, the tandem cell is slightly top cell limited. The initial efficiency of the micromorph cell is 12.04 %, Voc = 1.278 V, Jsc=13.67 mA/cm^2, FF = 0.68 [31]. After light soaking, the stabilised values are; η = 11.4 %, Voc = 1.279 V, Jsc = 13.61 mA/cm^2 and FF = 0.64 [31]. Thus, the degradation of the efficiency is only 5 % of its initial value, due to the decay in the fill factor. We attribute this to the degradation of the top cell, as the tandem is top cell limited (verified from the spectral response). We will in future attempt to increase the deposition rate so that the total deposition time of the i-layers in the tandem cell can be within 10 minutes.

4. Conclusions

Depositions of amorphous and microcrystalline silicon cells (which are essential components of "micromorph cells") by VHF PECVD at high deposition rates and acceptable efficiencies have been demonstrated. Among other techniques, only HWCVD has shown promise, especially in the deposition of a-Si:H cells at high rates.

References

[1] J. Meier, S. Dubail, R. Flückiger, D. Fischer, H. Keppner, A. Shah, Proceedings of First WCPEC, 1994, p 409.

[2] J. K. Rath, Sol. Energy Mater. Sol. Cells **76**, 431 (2003).

[3] C. A. M. Stap, H. Meiling, G. Landweer, J. Bezemer, W. F. van der Weg, Proc. 9th EC Photovoltaic Solar Energy Conference, Freiburg, 1989, p.74.

[4] A. Gordijn, J. Löffler, W. M. Arnoldbik, F. D. Tichelaar, J. K. Rath, R. E. I. Schropp, Sol. Energy Mater. Sol. Cells **87**, 445 (2005).

[5] R. W. Collins, A. S. Ferlauto, G. M. Ferreira, Chi Chen, Joohyun Koh, R. J. Koval, Yeeheng Lee, J. M. Pearce, C. R. Wronski, Sol. Energy Mater. Sol. Cells **78**, 143 (2003).

[6] H. Kawasaki, K. Sakamoto, S. Maeda, T. Fukuzawa, M. Shiratani, Y. Watanabe, Jpn. J. Appl. Phys. **37**, 5757 (1998).

[7] M. Heintze, R. Zedlitz, J. Non-Cryst. Solids **198-200**, 1038 (1996).

[8] T. Nishimoto, M. Takai, H. Miyahara, M. Kondo, A. Matsuda, J. Non-Cryst. Solids **299–302**, 1116 (2002).

[9] A. C. W. Biebericher, W. F. van der Weg, J. K. Rath, M. R. Akdim, W. J. Goedheer, J. Vac. Sci. Technol. A, **21,** 156 (2003).

[10] A. C. W. Biebericher, Ph.D. Thesis, Utrecht Univ. (2002).

[11] J. K. Rath, A.C.W. Biebericher, R. J Zambrano,.R.E.I. Schropp, W.F.Van Der Weg, W.J. Goedheer, Mater. Res. Soc. Symp. Proc. **715**, 577 (2002).

[12] J. K. Rath, A.C.W. Biebericher, R.E.I. Schropp, W.F.Van Der Weg, W.J. Goedheer, Proc. 3rd WCPEC B, 2003, p.1748.

[13] R. E. I. Schropp, M.K.Van Veen, C.H.M van der Werf, D.L.Williamson, A.H.Mahan, Mater. Res. Soc.. Symp. Proc. **808**, 425 (2004).

[14] R. H. Franken, C. H. M. van der Werf, J. Löffler, J. K. Rath, R. E. I. Schropp, Thin Solid Films **501**, 47 (2006).

[15] R. H. Franken, Hongbo Li, Robert Stolk, Karine van der Werf, Jatindra K. Rath, Ruud Schropp, Proc. WCPEC4, Hawaii, 2006 (in press).

[16] A. Petit, Ph.D.Thesis, TU Delft (2006).

[17] H. Kakiuchi, H. Ohmi, Y. Kuwahara, M. Matsumoto, Y. Ebata, K.Yasutake, K. Yoshii, Y. Mori, Jap. J. Appl. Phys. **45**, 3587 (2006).

[18] H. Takatsuka, M. Noda, Y. Yonekura, Y. Takeuchi, Y. Yamauchi, Solar Energy **77**, 951 (2004).

[19] Q. Wang, E. Iwaniczko, Y. Xu, B. P. Nelson, A. H. Mahan, Mater. Res. Soc. Symp. Proc. **557**, 163 (1999).

[20] M. Komoda, K Niira, H.Senta, T. Nishimura, H.Hakuma, H.Okui, K.Aramaki, Y.Okada, K.Tomita, H. Higuchi, H.Arimune, Proc. 3rd World Conf. on Photovoltaic Energy Conversion, Vol B, 2003, p. 1733.

[21] L. Guo, M. Kondo, M. Fukawa, K. Saitoh and A. Matsuda, Jap. J. Appl. Phys. **37**, L1116 (1998).

[22] J. K. Rath, F.D.Tichelaar, H. Meiling, R.E.I. Schropp, Mat. Res. Symp. Proc., **507**, 879 (1998).

[23] J. K. Rath, H. Meiling, R. E. I. Schropp, Jap. J. Appl. Phys. **36**, 5436 (1997).

[24] J. K. Rath, R. E. I. Schropp, W. Beyer, Diffusion and Defect Data Pt.B: Solid State Phenomena **80-81**, 109 (2001).

[25] J. K. Rath, K.F. Feenstra, D. Ruff, H. Meiling, R.E.I. Schropp, Mater Res. Soc. Symp. Proc. **452**, 977 (1997).

[26] J. K. Rath, F.A. Tichelaar, R.E.I. Schropp, Diffusion and Defect Data Pt.B: Solid State Phenomena **67**, 465 (1999).

[27] O. Vetterl, F. Finger, R. Carius, P. Hapke, L. Houben, O. Kluth, A. Lambertz, A. Muck, B. Rech and H. Wagner, Sol. Energy Mater. Sol. Cells **62**, 97 (2000).

[28] J. Meier, E. Vallat-Sauvain, S. Dubail, U. Kroll, J. Dubail, S. Golay, L. Feitknecht, P. Torres, S. Fay, D. Fischer, A. Shah, Sol. Energy Mater. Sol. Cells **66**, 73 (2001).

[29] A. Gordijn, J. Francke, L. Hodakova, J. K. Rath, R. E. I. Schropp, Mater. Res. Soc. Symp. Proc. **862**, 87 (2005).

[30] A. Gordijn, M. Vanecek, W. J. Goedheer, J. K. Rath, R. E. I. Schropp, Jap. J. Appl. Phys. **45**, 6166 (2006).
[31] A. Gordijn, J. K. Rath, R. E. I. Schropp, Progress in Photovoltaics: Research and Applications **14**, 305 (2006).
[32] J. K. Rath, R. H. J. Franken, A. Gordijn, R. E. I. Schropp, W. J. Goedheer, J. Non-Cryst. Solids **338–340**, 56 (2004).
[33] J. K. Rath, Arjan Verkerk, Ronald Franken, Caspar van Bommel, Karine van der Werf, Aad Gordijn, Ruud Schropp, Proc. WCPEC4, Hawaii, 2006 (in press).
[34] A. Gordijn, L. Hodakova, J. K. Rath, R. E. I. Schropp, J. Non-Cryst. Solids **352,** 1868 (2006).
[35] A. Gordijn, J. K. Rath, R.E.I.Schropp, Technical Digest, Int. PVSEC15, Sanghai, 2005, p.955.
[36] J. K. Rath, A.J. Hardeman, C.H.M. van der Werf, P.A.T.T. van Veenendaal, M.Y.S. Rusche, R.E.I. Schropp, Proc. WCPEC3, Osaka, Japan, 2003, p.1562.

*Corresponding author: J.K.Rath@phys.uu.nl